







# Optical fiber point sensors based on forward Brillouin scattering

KEREN SHEMER,<sup>1</sup> GIL BASHAN,<sup>1</sup> ELAD ZEHAVI,<sup>1</sup> HILEL HAGAI DIAMANDI,<sup>1,2</sup> ALON BERNSTEIN,<sup>1</sup> KAVITA SHARMA,<sup>1</sup> YOSEF LONDON,<sup>1,3</sup> DAVID BARRERA,<sup>4</sup>  SALVADOR SALES,<sup>4</sup>  ARIK BERGMAN,<sup>1,5</sup>  AND AVI ZADOK<sup>1,\*</sup> 

<sup>1</sup>Faculty of Engineering and Institute for Nano-Technology and Advanced Materials, Bar-Ilan University, Ramat-Gan 5290002, Israel

<sup>2</sup>Currently with the Department of Computer Science and Applied Mathematics, Weizmann Institute of Science, Rehovot 7610001, Israel

<sup>3</sup>Currently with the Applied Physics Division, Soreq NRC, Yavne 81800, Israel

<sup>4</sup>Photonics Research Labs, iTEAM Research Institute, Universitat Politècnica de València, 46022 Valencia, Spain

<sup>5</sup>Currently with the Department of Electrical and Electronic Engineering, Milken Campus, Ariel University, Ariel 40700, Israel

\*Avinoam.Zadok@biu.ac.il

**Abstract:** Forward Brillouin scattering interactions support the sensing and analysis of media outside the cladding boundaries of standard fibers, where light cannot reach. Quantitative point-sensing based on this principle has yet to be reported. In this work, we report a forward Brillouin scattering point-sensor in a commercially available, off-the-shelf multi-core fiber. Pump light at the inner, on-axis core of the fiber is used to stimulate a guided acoustic mode of the entire fiber cross-section. The acoustic wave, in turn, induces photoelastic perturbations to the reflectivity of a Bragg grating inscribed in an outer, off-axis core of the same fiber. The measurements successfully analyze refractive index perturbations on the tenth decimal point and distinguish between ethanol and water outside the centimeter-long grating. The measured forward Brillouin scattering linewidths agree with predictions. The acquired spectra are unaffected by forward Brillouin scattering outside the grating region. The results add point-analysis to the portfolio of forward Brillouin scattering optical fiber sensors.

© 2022 Optica Publishing Group under the terms of the [Optica Open Access Publishing Agreement](#)

## 1. Introduction

Point-measurement of a quantity of interest is the most common form of optical fiber sensing. The most widely employed sensor elements are short-period fiber Bragg gratings (FBGs) [1]. The wavelengths of peak reflectivity of FBGs vary with temperature and axial strain [2]. FBGs are also used for indirect monitoring of other metrics through intermediate transduction mechanisms [3]. For example, humidity can be measured based on the strain induced to an FBG by the swelling of a polyimide coating layer [4]. FBGs in etched or tapered fibers can be sensitive to the refractive index of surrounding media through the evanescent tails of optical modes [5,6]. The gratings also serve in refractive index measurements outside the fiber, based on the coupling of guided light to cladding modes [7]. However, the spectra of FBGs reflectivities are generally insensitive to the elastic properties of test substances outside standard silica fibers, unless further structural modifications are applied.

Forward Brillouin scattering is an opto-mechanical interaction between optical field components and guided acoustic modes that co-propagate in a common medium [8]. Acoustic waves are stimulated by optical fields through the mechanism of electrostriction, and the same waves are monitored via photoelastic scattering of light [8]. Unlike the more widely known backward

scattering effect, the acoustic modes that take part in forward Brillouin scattering in standard fibers span the entire cross-section of the cladding and reach its boundaries [8]. The forward scattering process is therefore dependent on the elastic properties of outside media. That dependence serves as the basis for a new category of forward Brillouin fiber sensors, first proposed and demonstrated in 2016 [9].

Monitoring of forward Brillouin scattering spectra supports quantitative analysis of liquids outside the fiber cladding and even outside its coating layers [9–11], as well as analysis of the coating layers themselves [12]. Most protocols reported to-date have been position-integrated: Forward Brillouin scattering spectra were accumulated over the entire length of a fiber under test [9–13]. While such accumulative measurements can be precise and sensitive, they cannot resolve localized information. Starting in 2018, several concepts for the spatially distributed analysis of forward Brillouin scattering have been proposed and demonstrated as well [14–17]. An impressive spatial resolution of less than a meter has been recently achieved [17]. However, quantitative point-sensing based on forward Brillouin scattering has yet to be demonstrated: The most basic form of measurement has been missing in this new and promising category of optical fiber sensors.

In an earlier work, we were able to distinguish between air and liquid outside the cladding of a centimeter-long multi-core fiber (MCF) section using forward Brillouin scattering [18]. A guided acoustic mode of the fiber was stimulated by light at the inner, on-axis core of the fiber. The acoustic wave was monitored through photoelastic perturbations to the reflectivity of a short FBG that was inscribed in an outer, off-axis core. The photoelastic perturbations induced intensity modulation to a probe wave reflected from the grating. However, quantitative analysis and distinction between different liquids could not be obtained, due to pronounced background of photoelastic scattering outside the point of interest [18].

In this work, we report the quantitative analysis of local forward Brillouin scattering spectra of a centimeter-long section of a commercially available, off-the-shelf seven core fiber. The method previously used in [18] is substantially improved upon. With careful choice of the FBG location, the output probe modulation becomes insensitive to forward Brillouin scattering outside the short grating region. The measurements successfully analyze photoelastic perturbations to the local refractive index in the tenth decimal point. The results distinguish between air, water, and ethanol outside the cladding at the location of the grating. The observed spectral linewidths for the three media agree with expectations. The protocol extends the portfolio of forward Brillouin optical fiber sensors. Preliminary results were briefly reported in a recent conference [19].

## 2. Principle of operation

Consider an acoustic mode of radial symmetry  $R_{0m}$ , where  $m$  is an integer, which is guided along the axis of an MCF. The mode is characterized by its cut-off frequency  $\Omega_{0m}$ , on the order of hundreds of MHz, and by its radial displacement profile  $u_{0m}(r)$  [ $\text{m}^{-1}$ ] where  $r$  is the transverse radial coordinate. The profile is normalized so that  $2\pi \int_0^a |u_{0m}(r)|^2 r dr = 1$ , with  $a$  the cladding radius [8,20]. The mode is stimulated by polarized pump light that is propagating in the on-axis core of the MCF in the positive  $\hat{z}$  direction, from  $z = 0$ . The pump wave is intensity modulated at a radio frequency  $\Omega \approx \Omega_{0m}$ . We denote the magnitude [W] of the pump power modulation as  $P_p(\Omega)$ . The pump wave induces an electrostrictive force per unit volume [8,21], which includes a radial term with radially symmetric magnitude [8,21]. That force term can drive the oscillations of radial guided acoustic modes. The stimulated modal displacement is given by  $b_{0m}(\Omega, z)u_{0m}(r)$ , with a modal magnitude [ $\text{m}^2$ ], [8,20]:

$$b_{0m}(\Omega, z) = \frac{1}{4nc\rho_0} Q_{0m}^{(ES)} \frac{1}{\Omega_{0m}^2 - \Omega^2 - j\Omega\Gamma_{0m}(z)} P_p(\Omega). \quad (1)$$

Here  $\rho_0$  denotes the density of silica,  $n$  is its refractive index, and  $c$  is the speed of light in vacuum. Electrostrictive stimulation is the most efficient at acoustic frequencies  $\Omega$  close to the modal cut-off  $\Omega_{0m}$ .  $Q_{0m}^{(ES)}$  represents the spatial overlap integral between the transverse profile of the electrostrictive driving force and that of the modal displacement [8,21]. It is explicitly given by [8,20]:

$$Q_{0m}^{(ES)} = -2\pi(a_1 + 2a_2) \int_0^a \frac{\partial E_T(r)}{\partial r} E_T(r) u_{0m}(r) r dr. \quad (2)$$

In Eq. (2),  $E_T(r)$  [ $\text{m}^{-1}$ ] is the radial profile of the optical field in the inner core of the fiber, normalized so that  $2\pi \int_0^a |E_T(r)|^2 r dr = 1$ , and  $a_1 = 0.66$ ,  $a_2 = -1.19$  are photoelastic parameters of silica. Lastly,  $\Gamma_{0m}(z)$  in Eq. (1) represents the linewidth of the acoustic mode at position  $z$ . The linewidth also signifies the decay rate of acoustic intensity, and it is determined by the local mechanical impedance  $Z_{out}(z)$  outside the cladding [9]:

$$\Gamma_{0m}(z) = \Gamma_{0m}^{(int)} - \frac{v_L}{a} \ln \left[ \frac{Z_{out}(z) - Z_{in}}{Z_{out}(z) + Z_{in}} \right]. \quad (3)$$

Here  $v_L$  is the velocity of dilatational acoustic waves in silica,  $Z_{in}$  denotes the mechanical impedance of silica, and  $\Gamma_{0m}^{(int)}$  is the decay rate due to acoustic dissipation in silica. The first term of Eq. (3) dominates when a bare fiber is kept in air, whereas the second term is the more significant when the fiber is coated or immersed in liquid. The above relation provides the basis of opto-mechanical fiber sensing of media outside the cladding boundary [9–17]. For brevity, we define below:  $H(\Omega, z) \equiv 1/[\Omega_{0m}^2 - \Omega^2 - j\Omega\Gamma_{0m}(z)]$ . The stimulated acoustic wave propagates along the fiber axis  $\hat{z}$  with frequency  $\Omega$  and axial wavenumber  $K = n\Omega/c$  [8]. The stimulation of radial acoustic modes is independent of the state of polarization of the pump wave [22].

Material displacement of the acoustic mode is associated with strain in the medium. Strain, in turn, modifies the local dielectric tensor at every location within the fiber due to photoelasticity. The dielectric perturbations are in overlap with all cores of the MCF [20], not only with the on-axis core in which the pump light is launched, and they propagate along the fiber with frequency  $\Omega$  and wavenumber  $K$ . We consider next an outer core, whose center is offset from the fiber axis by a transverse vector  $\vec{r}_0$ . The effective refractive index seen by light guided in that core in position  $z$  is oscillating at frequency  $\Omega$ , with a magnitude that depends on its state of polarization. Light that is linearly polarized along  $\vec{r}_0$  is subject to refractive index perturbations of approximate magnitude:

$$\overline{\Delta n_{0m}^{(PE,1)}}(\Omega, z) \approx \frac{Q_{0m}^{(PE,1)} b_{0m}(\Omega, z)}{2n}, \quad (4)$$

where we have defined [20]:

$$Q_{0m}^{(PE,1)} \approx \int_0^a \int_0^{2\pi} \left[ (a_1 + a_2) \frac{\partial u_{0m}(r)}{\partial r} + a_2 \frac{u_{0m}(r)}{r} \right] |E_T(|\vec{r} - \vec{r}_0|)|^2 d\phi r dr. \quad (5)$$

Here  $\vec{r}$  denotes a vector in the transverse plane and  $\phi$  is the transverse azimuthal coordinate. Light of the orthogonal linear polarization in the same core undergoes photoelastic refractive index perturbations of a different magnitude [20]:

$$\overline{\Delta n_{0m}^{(PE,2)}}(\Omega, z) \approx \frac{Q_{0m}^{(PE,2)} b_{0m}(\Omega, z)}{2n}, \quad (6)$$

$$Q_{0m}^{(PE,2)} \approx \int_0^a \int_0^{2\pi} \left[ a_2 \frac{\partial u_{0m}(r)}{\partial r} + (a_1 + a_2) \frac{u_{0m}(r)}{r} \right] |E_T(|\vec{r} - \vec{r}_0|)|^2 d\phi r dr. \quad (7)$$

We next consider an optical probe that is launched into the outer core from the opposite end  $z = L$  and propagates in the  $-\hat{z}$  direction. We examine the reflection of that probe wave from

an FBG located in the outer core at  $z = z_{FBG}$ . The effect of the stimulated acoustic mode  $R_{0m}$  on the intensity of the reflected probe wave is two-fold. First, in propagation over the section of fiber of length  $d_{FBG} = L - z_{FBG}$ , from its launch point until the grating position, the probe may accumulate photoelastic phase modulation [8,21]. Such phase modulation might then be converted into intensity modulation upon reflection from the grating. Such conversion of phase to intensity is undesirable for the purpose of this study, since it does not represent local scattering at the point of the grating. However, since the stimulated acoustic wave and the probe are counter-propagating, the photoelastic phase modulation of the probe is subject to wavenumbers mismatch of  $\Delta k = 2K$  [8,21]. If the path length  $d_{FBG}$  equals an integer multiple of the period  $D_{0m} \equiv 2\pi c / (n\Omega_{0m})$ , the accumulated photoelastic phase modulation of the probe wave reaching  $z_{FBG}$  cancels out completely. In this case, the reflection of the probe wave from the FBG is unaffected by forward Brillouin scattering along the fiber section leading to the grating.

The second effect of the acoustic wave on the reflected probe takes place via perturbations to the grating reflectivity, which is modified by the oscillations of the local refractive index with magnitude  $\overline{\Delta n_{0m}^{(PE,i)}}(\Omega, z_{FBG})$ . Here  $i = 1, 2$  refer to the choice of probe polarization state. The Bragg wavelength varies in time at frequency  $\Omega$ , and the reflectivity spectrum of the grating is offset back and forth accordingly. A probe wave of fixed wavelength, chosen on a spectral slope of the grating reflectivity spectrum, would therefore experience a reflectivity that changes with time at the same frequency  $\Omega$ . The magnitude of reflectivity oscillations would scale with that of the local refractive index perturbations.  $\overline{\Delta n_{0m}^{(PE,i)}}(\Omega, z_{FBG})$ . The magnitude  $\delta P_s^{(i)}(\Omega)$  [W] of the reflected probe modulation is given by:

$$\begin{aligned} \delta P_s^{(i)}(\Omega) &\approx Q_{FBG} \mathfrak{R}_{max} P_s \frac{\overline{\Delta n_{0m}^{(PE,i)}}(\Omega, z_{FBG})}{n} \\ &= \frac{Q_{0m}^{(ES)} Q_{0m}^{(PE,i)} Q_{FBG}}{8n^3 c \rho_0} \cdot \mathfrak{R}_{max} P_s \cdot H(\Omega, z_{FBG}) P_p(\Omega). \end{aligned} \quad (8)$$

In Eq. (8),  $Q_{FBG}$  and  $\mathfrak{R}_{max}$  denote the quality factor and the maximum of the FBG power reflectivity spectrum, respectively, and  $P_s$  is the input power of the probe wave. An incident probe wave can be aligned with the state of polarization for which the refractive index perturbations are larger [20]. The transfer function between the power modulation  $P_p(\Omega)$  of the input pump wave and that of the reflected probe  $\delta P_s^{(i)}(\Omega)$  is proportional to  $H(\Omega, z_{FBG})$  and may retrieve the mechanical impedance of an outside medium. The results would represent point-measurements, as they are only affected by conditions at the location of the FBG. The reflected probe wave undergoes further phase modulation by the stimulated acoustic waves over a length  $d_{FBG}$  before reaching the end of the fiber, however that phase modulation contribution is not converted to an intensity reading. Note that the inscription of the grating in the outer core is mandatory: without the grating, the local perturbations to the refractive index would not manifest as intensity modulation of the probe wave.

The pump and probe waves are separated both spectrally and spatially, so that the leakage of modulating signals between them is strongly suppressed. For example, the Kerr effect does not contribute to cross-phase modulation between pump and probe in different cores. Drifting of the grating wavelength of peak reflectivity, on a wider scale than the reflectivity bandwidth, could potentially lead to misinterpretation of experimental data. However, such drifting is unlikely to occur within the short experimental duration (see Section 3).

The refractive index perturbation magnitudes  $\overline{\Delta n_{0m}^{(PE,i)}}(\Omega, z_{FBG})$ , at the acoustic resonance frequencies  $\Omega_{0m}$  and for 1 W pump power, are only on the order of  $10^{-9}$  -  $10^{-10}$  refractive index units (RIU), depending on the medium outside the cladding [18,20]. The intensity modulation depth of the reflected probe wave,  $\delta P_s^{(i)}(\Omega)/P_s$ , is typically between 1-10 ppm. As seen in Eq. (8),

the use of an FBG with a narrower reflectivity spectrum (larger  $Q_{FBG}$ ) would yield a larger modulation signal. The measurements of such small signals can be challenging. Nevertheless, the proposed method has been successfully demonstrated as described next.

### 3. Experimental setup and results

The experimental setup for point-measurements of forward Brillouin scattering spectra is illustrated in Fig. 1. Pump light was drawn from a 1550 nm wavelength laser diode. The intensity of the pump was modulated by a sine wave of variable radio frequency  $\Omega$  from the output port of a vector network analyzer. The frequency  $\Omega$  was scanned in the vicinity of the cut-off frequency  $\Omega_{06}$  of radial guided acoustic mode  $R_{06}$ . The sine waveform was applied to a Mach-Zehnder electro-optic intensity modulator. The modulation depth of the pump wave intensity was close to 1. The modulated pump wave was amplified to an average power of 600 mW and launched into the inner, on-axis core of a seven-core fiber in the positive  $\hat{z}$  direction, at  $z = 0$ .

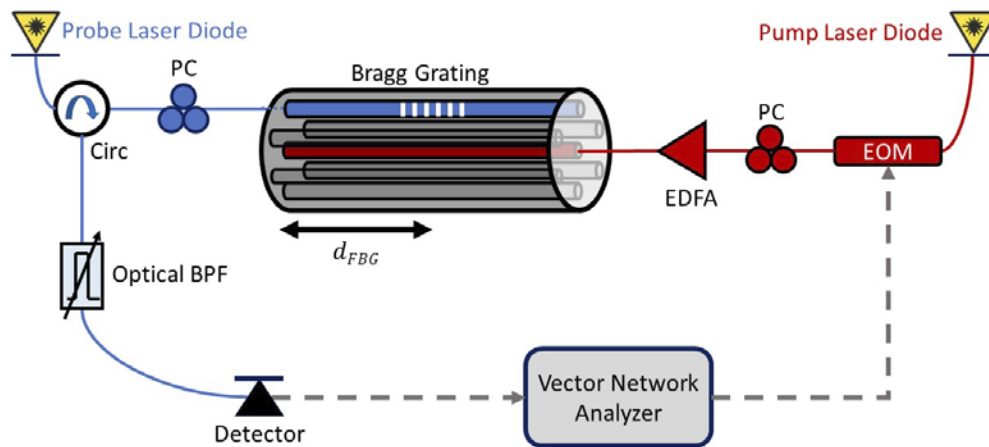


**Fig. 1.** Schematic illustration of the experimental setup used in forward Brillouin point-sensing outside the cladding of a multi-core fiber [19]. EDFA: erbium-doped fiber amplifier; EOM: Mach-Zehnder electro-optic intensity modulator; PC: polarization controller; BPF: bandpass filter; Circ: circulator. Modulated pump light is coupled to the inner core of the fiber and stimulates a radial guided acoustic mode. The acoustic wave is monitored through photoelastic perturbations to the reflection of a probe wave from a grating inscribed in the outer core. Pump and probe are launched from opposite ends. The grating is located at a distance  $d_{FBG}$  of 70 cm from the probe input end of the probe wave (see text).

The cladding diameter of the fiber under test was 125  $\mu\text{m}$ , and its six outer cores were located on a hexagonal grid with 35  $\mu\text{m}$  separation. The mode field diameters of light guided in all seven cores were 6.1  $\mu\text{m}$ . The length  $L$  of the fiber was 7 m. The fiber was coated by standard dual-layer acrylate coating. Insertion losses of optical power through the fan-in and fan-out units at the ends of the MCF were specified as 0.5 dB per interface, and the inter-core crosstalk of optical power was specified as  $-50$  dB. The pump wave stimulated radial guided acoustic modes of the MCF as discussed in Section 2. A polarization controller was used to inhibit the electrostrictive stimulation of torsional-radial guided acoustic modes at the point of measurement [22].

Continuous probe light from a second, tunable laser diode was launched into an outer core of the MCF, in the negative  $-\hat{z}$  direction, from  $z = L$ . The optical power of the probe wave was 20 mW. The probe light was coupled to the fiber through a circulator. An FBG was inscribed in the outer core of the fiber [23]. The coating was removed from a centimeter-long section containing the grating prior to its inscription, and that section remained uncoated. The fiber remained

coated along the rest of its length. The wavelength and magnitude of the FBG peak power reflectivity were 1548.5 nm and 0.6, respectively. The quality factor of the grating reflectivity spectrum was 20,000. The exact wavelength of the probe was adjusted to a slope of the grating reflectivity spectrum. Photoelastic perturbations due to the stimulated acoustic waves modulated the instantaneous intensity of the reflected probe wave as discussed above. A polarization controller was used to adjust the state of polarization of the probe wave for maximum photoelastic modulation.

The FBG was inscribed at a distance  $d_{FBG} = 70 \pm 1$  cm from the end of the fiber  $z = L$ . The optimal distance  $D_{06}$  for the cancellation of photoelastic phase modulation of the probe at the frequencies  $\Omega$  of interest is 75 cm (see Section 2). While  $d_{FBG}$  deviated from the optimal  $D_{06}$  by a few centimeters, the phase modulation of the probe wave prior to its reflection from the FBG was nevertheless largely suppressed. The reflected probe wave was detected by a photo-receiver of 1 GHz bandwidth, responsivity of  $50,000 \text{ V} \times \text{W}^{-1}$ , and noise-equivalent power of  $16 \times 10^{-12} \text{ W} \times \text{Hz}^{-0.5}$ . The thermal noise of the receiver was the dominant source of noise in the measurement of the output probe wave modulation. A tunable optical bandpass filter was used to block residual leakage of the pump wave from reaching the receiver. The relative rejection ratio of the filter at the pump wavelength was  $-35$  dB. Altogether, the relative crosstalk of the pump wave between the fiber input and the photo-receiver was  $-85$  dB.

Figure 2 shows measured transfer functions of radio frequency electrical power between the modulation of the input pump wave and that of the detected, reflected probe wave (solid lines). The transfer functions are proportional to  $|H(\Omega, z_{FBG})|^2$ . Traces were acquired with the FBG

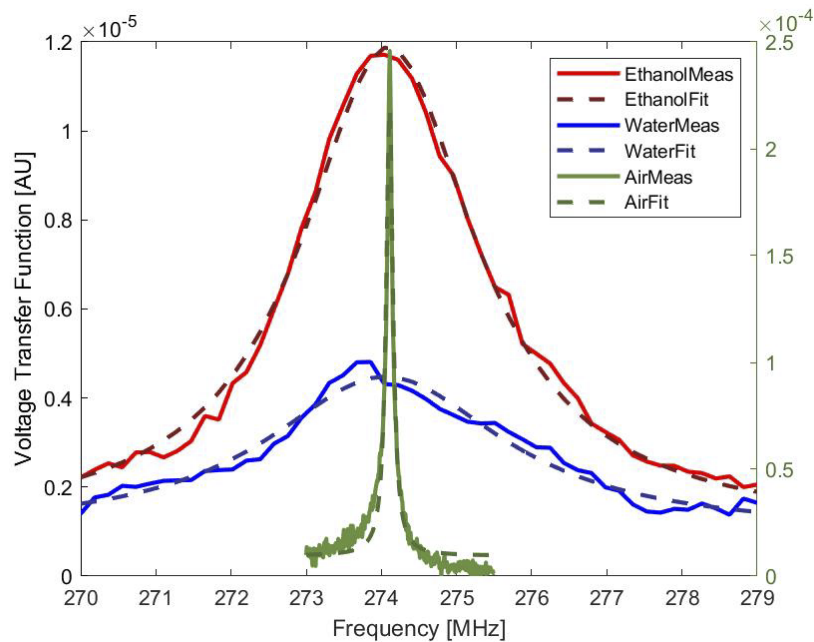


**Fig. 2.** Transfer functions of radio frequency electrical power between the modulation of the input pump wave and that of the detected probe wave following reflection from the grating (see legend). Green: the 1 cm-long fiber section containing the grating was exposed to air. In the red (blue) trace, the same section was immersed in ethanol (doubly distilled water). Solid lines represent the average of five acquired traces, and dashed lines show the corresponding Lorentzian fits. Traces for the grating in ethanol and water refer to the left-hand vertical axis. Traces for the grating in air relate to the right-hand vertical axis.

in air (green) or immersed in ethanol (red) or doubly distilled water (blue). When the grating was in air, the modulation frequency of the pump wave was scanned between 273 MHz and 275.5 MHz at 8 kHz increments, and the measurement bandwidth of the network analyzer was 500 Hz. When the grating was immersed in liquids, the modulation frequency was scanned between 270 MHz and 279 MHz at 180 kHz steps, and the measurement bandwidth was reduced to 3 Hz. The acquisition duration of each trace with liquids outside the grating was 17 seconds. Measurements with liquids outside the grating were averaged over 5-10 repeating traces. Drifting of the FBG wavelength of peak reflectivity within that acquisition duration was much smaller than the reflectivity bandwidth. The dashed lines show fitted Lorentzian line shapes of the measured traces. A resonant response due to photoelastic perturbations by radial guided acoustic mode  $R_{06}$  is observed in all traces, near 274 MHz frequency. The full widths at half maximum of the measured resonances were  $100 \pm 8$  kHz,  $2.85 \pm 0.1$  MHz, and  $3.85 \pm 0.35$  MHz, with the FBG in air, ethanol, or water, respectively. The experimental uncertainties represent the standard deviations among repeating acquisitions in each medium. The measured linewidth in air signifies  $\Gamma_{06}^{(int)}$ .

The results successfully distinguish among the three media outside the cm-long grating. The linewidth of the acoustic wave stimulation is broader with water outside the cladding due to its higher mechanical impedance, compared with that of ethanol [9]. In addition, the maximum modulation of the probe wave with the grating in ethanol (water) is 20 (60) times weaker than with the grating in air. The expected modal linewidths for a bare fiber in ethanol and water are 2.3 MHz and 3.55 MHz, respectively [11]. These estimates include the contribution of  $\Gamma_{06}^{(int)}$ . The measured linewidths are in general agreement with predictions.

#### 4. Summary and conclusions

Quantitative point-measurements of forward Brillouin scattering spectra were performed in a commercially available, off-the-shelf MCF. Acoustic waves were stimulated by pump light in the inner core of the fiber, and they were monitored through photoelastic perturbations to the reflectivity of an FBG in an outer core. Pump and probe waves were separated both spatially and spectrally to reduce crosstalk. The measurements successfully characterized modulation to the local refractive index in the tenth decimal point. The measured spectra distinguished between air, ethanol, and water outside the centimeter-long grating. The observed linewidths of forward Brillouin scattering were in general agreement with expectations: The differences between model and experiment were 20% for ethanol outside the cladding, and 10% for water. The disagreement for water is within experimental uncertainty. Differences could be due to micron-scale residues of the acrylate coating that were not fully removed from the fiber cladding at the grating region [11,12]. At this time, we could not validate or disprove this possibility in a non-destructive manner.

The results improve upon our earlier study [18], which only obtained qualitative distinction between air and liquid outside the MCF cladding. Accumulated photoelastic phase modulation of the probe wave along the fiber, which restricted our earlier work, was successfully cancelled by judicious choice of the grating position with respect to the end of the fiber. The measurement protocol can be cascaded to quasi-distributed analysis using multiple gratings in series. The locations of the gratings would be limited to integer multiples of the optimal distance  $D_{0m}$  from the input end of the probe wave. This limitation can be relaxed using multiple acoustic modes of different cut-off frequencies  $\Omega_{0m}$ , and hence different values of  $D_{0m}$ . The results extend forward Brillouin optical fiber sensors to include quantitative point-analysis. Future work would include the use of coated gratings, multiplexing of gratings in series, and mechanical impedance measurements with higher precision.

**Funding.** Bar-Ilan University.

**Disclosures.** The authors declare no conflict of interest.

**Data availability.** Data underlying the results presented in this paper are not publicly available at this time but may be obtained from the authors upon reasonable request.

## References

1. R. Kashyap. *Fiber Bragg Gratings*. Academic (2009).
2. H. J. Patrick, G. M. Williams, A. D. Kersey, J. R. Pedrazzani, and A. M. Vengsarkar, "Hybrid fiber Bragg grating/long period fiber grating sensor for strain/temperature discrimination," *IEEE Photonics Technol. Lett.* **8**(9), 1223–1225 (1996).
3. Y. J. Rao, "Recent progress in applications of in-fibre Bragg grating sensors," *Optics and Lasers in Engineering* **31**(4), 297–324 (1999).
4. P. Kronenberg, P. K. Rastogi, P. Giaccari, and H. G. Limberger, "Relative humidity sensor with optical fiber Bragg gratings," *Opt. Lett.* **27**(16), 1385–1387 (2002).
5. A. Asseh, S. Sandgren, H. Ahlfeldt, B. Sahlgren, R. Stubbe, and G. Edwall, "Fiber Optical Bragg Grating Refractometer," *Fiber Integr. Opt.* **17**(1), 51–62 (1998).
6. A. N. Chryssis, S. M. Lee, S. B. Lee, S. S. Saini, and M. Dagenais, "High sensitivity evanescent field fiber Bragg grating sensor," *IEEE Photon. Technol. Lett.* **17**(6), 1253–1255 (2005).
7. S. W. James and R. P. Tatam, "Optical fibre long-period grating sensors: characteristics and application," *Meas. Sci. Technol.* **14**(5), R49–R61 (2003).
8. R. M. Shelby, M. D. Levenson, and P. W. Bayer, "Guided acoustic-wave Brillouin scattering," *Phys. Rev. B* **31**(8), 5244–5252 (1985).
9. Y. Antman, A. Clain, Y. London, and A. Zadok, "Optomechanical sensing of liquids outside standard fibers using forward stimulated Brillouin scattering," *Optica* **3**(5), 510–516 (2016).
10. D. M. Chow and L. Thévenaz, "Forward Brillouin scattering acoustic impedance sensor using thin polyimide-coated fiber," *Opt. Lett.* **43**(21), 5467–5470 (2018).
11. H. H. Diamandi, Y. London, G. Bashan, and A. Zadok, "Distributed opto-mechanical analysis of liquids outside standard fibers coated with polyimide," *APL Photonics* **4**(1), 016105 (2019).
12. H. H. Diamandi, Y. London, G. Bashan, K. Shemer, and A. Zadok, "Forward Stimulated Brillouin Scattering Analysis of Optical Fibers Coatings," *J. Lightwave Technol.* **39**(6), 1800–1807 (2021).
13. N. Hayashi, Y. Mizuno, K. Nakamura, S. Y. Set, and S. Yamashita, "Experimental study on depolarized GAWBS spectrum for optomechanical sensing of liquids outside standard fibers," *Opt. Express* **25**(3), 2239–2244 (2017).
14. D. Chow, Z. Yang, M. A. Soto, and L. Thévenaz, "Distributed forward Brillouin sensor based on local light phase recovery," *Nat. Commun.* **9**(1), 2990 (2018).
15. G. Bashan, H. H. Diamandi, Y. London, E. Preter, and A. Zadok, "Optomechanical time-domain reflectometry," *Nat. Commun.* **9**(1), 2991 (2018).
16. C. Pang, Z. Hua, D. Zhou, H. Zhang, L. Chen, X. Bao, and Y. Dong, "Opto-mechanical time-domain analysis based on coherent forward stimulated Brillouin scattering probing," *Optica* **7**(2), 176–184 (2020).
17. S. Zaslowski, Z. Yang, and L. Thévenaz, "Distributed optomechanical fiber sensing based on serrodyne analysis," *Optica* **8**(3), 388–395 (2021).
18. H. H. Diamandi, Y. London, A. Bergman, G. Bashan, J. Madrigal, D. Barrera, S. Sales, and A. Zadok, "Opto-mechanical interactions in multi-core optical fibers and their applications," invited paper, *IEEE J. Sel. Top. Quantum Electron.* **26**(4), 1–13 (2020).
19. K. Shemer, G. Bashan, E. Zehavi, H. H. Diamandi, A. Bernstein, K. Sharma, Y. London, D. Barrera, S. Sales, and A. Zadok, "Forward Brillouin Point Sensor in a Multi-Core Fiber," paper Th4.67, *27th Optical Fiber Sensors Conference (OFS)*, Proc. Optica Publishing Group (2022).
20. H. H. Diamandi, Y. London, and A. Zadok, "Opto-mechanical inter-core cross-talk in multi-core fibers," *Optica* **4**(3), 289–297 (2017).
21. M. S. Kang, A. Brenn, and P. St. J. Russell, "All-optical control of gigahertz acoustic resonances by forward stimulated interpolarization scattering in a photonic crystal fibre," *Phys. Rev. Lett.* **105**(15), 153901 (2010).
22. H. H. Diamandi, G. Bashan, Y. London, K. Sharma, K. Shemer, and A. Zadok, "Interpolarization Forward Stimulated Brillouin Scattering in Standard Single-Mode Fibers," *Laser Photonics Rev.* **16**(1), 2100337 (2022).
23. I. Gasulla, D. Barrera, J. Hervas, and S. Sales, "Spatial division multiplexed microwave signal processing by selective grating inscription in homogeneous multicore fibers," *Sci. Rep.* **7**(1), 41727 (2017).